

Pressure-Driven Demand and Leakage Simulation for Water Distribution Networks

Orazio Giustolisi¹; Dragan Savic²; and Zoran Kapelan³

Abstract: Increasingly, water loss via leakage is acknowledged as one of the main challenges facing water distribution system operations. The consideration of water loss over time, as systems age, physical networks grow, and consumption patterns mature, should form an integral part of effective asset management, rendering any simulation model capable of quantifying pressure-driven leakage indispensable. To this end, a novel steady-state network simulation model that fully integrates into a classical hydraulic representation, pressure-driven demand and leakage at the pipe level is developed and presented here. After presenting a brief literature review about leakage modeling, the importance of a more realistic simulation model allowing for leakage analysis is demonstrated. The algorithm is then tested from a numerical standpoint and subjected to a convergence analysis. These analyses are performed on a case study involving two networks derived from real systems. Experimentally observed convergence/error statistics demonstrate the high robustness of the proposed pressure-driven demand and leakage simulation model.

DOI: 10.1061/(ASCE)0733-9429(2008)134:5(626)

CE Database subject headings: Water distribution system; Leakages; Water pipelines; Deterioration; Pipe networks.

Introduction

Water loss via leakage constitutes a major challenge to the effective operation of municipal distribution networks since it represents not only diminished revenue for utilities, but also undermined service quality (Almandoz et al. 2005) and wasted energy resources (Colombo and Karney 2002). A typical leakage control program usually starts with a water audit based on available flow measurements. Although this is an important first step, most practical studies do not go beyond it. In order to assist in leakage reduction and conduct more accurate analysis, a hydraulic model capable of accounting for pressure-driven (also known as head-driven) demand and leakage flow at pipe level should prove invaluable, and extended period simulation should be involved.

In fact, an integral part of any medium- to long-term rehabilitation planning for a water distribution system should be the analysis of pipe deterioration and the corresponding increase in water loss. In order to obtain a better estimate of flow through the network (with respect to both satisfied demand and losses through leakage), a pressure-driven hydraulic model is needed. Several models have been developed to incorporate pressure-driven de-

mand analysis into network reliability evaluation (Chandapillai 1991; Gupta and Bhawe 1996; Ackley et al. 2001; Kalungi and Tanyimboh 2003; Wu et al. 2006). This paper introduces a new simulation model that fully integrates a classic hydraulic simulation algorithm, such as that of Todini and Pilati (1988) found in EPANET 2 (Rossman 2000), with a pressure-driven model that entails a more realistic representation of leakage (Germanopoulos 1985; Germanopoulos and Jowitt 1989). The novel pressure-driven algorithm uses the framework of Todini's simulation model (Todini 2003) in order to account for pressure-driven leakage at the pipe level and offer a more realistic representation.

Pressure-Driven Demand/Leakage Network Simulation Model

The pressure-driven simulation of a network comprising n_p pipes with unknown discharges (i.e., flow rates), n_n nodes with unknown heads (internal nodes or junctions in the EPANET terminology), and n_0 nodes with known heads (tank levels, for example) can be described as in Todini (2003). Therefore, assuming the elements of the diagonal matrix \mathbf{A}_{pp} of order n_p equal to $R_k|Q_k|^{n-1}$, the pressure-driven simulation of a network can be described by the following system of equations based on energy and mass balance conservation:

$$\begin{bmatrix} \mathbf{A}_{pp} & \mathbf{A}_{pn} \\ \mathbf{A}_{np} & \mathbf{A}_{nn} \end{bmatrix} \begin{bmatrix} \mathbf{Q} \\ \mathbf{H} \end{bmatrix} = \begin{bmatrix} -\mathbf{A}_{p0}\mathbf{H}_0 \\ \mathbf{0} \end{bmatrix} \quad (1)$$

where $\mathbf{Q}=[Q_1, Q_2, \dots, Q_{n_p}]^T=[n_p, 1]$ column vector of unknown pipe flow rates; $\mathbf{H}=[H_1, H_2, \dots, H_{n_n}]^T=[n_n, 1]$ column vector of unknown nodal heads; $\mathbf{H}_0=[H_{01}, H_{02}, \dots, H_{0n_0}]^T=[n_0, 1]$ column vector of known nodal heads.

In the system of Eq. (1), $\mathbf{A}_{pn}=\mathbf{A}_{np}^T$ and \mathbf{A}_{p0} are topological incidence submatrices of size (n_p, n_n) and (n_p, n_0) , respectively, derived from the general topological matrix $\bar{\mathbf{A}}_{pn}=[\mathbf{A}_{pn}|\mathbf{A}_{p0}]$ of size $[n_p, n_n+n_0]$, as defined in (Todini 2003).

¹Professor, Dean, II Engineering Faculty, Dept. of Civil and Environmental Engineering, Technical Univ. of Bari, via Turismo, 8, 74100 Taranto, Italy (corresponding author). E-mail: o.giustolisi@poliba.it

²Professor, Centre for Water Systems, Univ. of Exeter, Harrison Building, North Park Rd., EX4 4QF Exeter, U.K. E-mail: d.savic@ex.ac.uk

³Senior Lecturer, Centre for Water Systems, Univ. of Exeter, Harrison Building, North Park Rd., EX4 4QF Exeter, U.K. E-mail: z.kapelan@ex.ac.uk

Note. Discussion open until October 1, 2008. Separate discussions must be submitted for individual papers. To extend the closing date by one month, a written request must be filed with the ASCE Managing Editor. The manuscript for this paper was submitted for review and possible publication on January 19, 2007; approved on September 10, 2007. This paper is part of the *Journal of Hydraulic Engineering*, Vol. 134, No. 5, May 1, 2008. ©ASCE, ISSN 0733-9429/2008/5-626-635/\$25.00.

In order to account for leakage flow rates in model (1), \mathbf{A}_{nn} can be cast as a diagonal matrix whose elements are the scalar product (i.e., element by element product) $-(\mathbf{q}_{act} + \mathbf{q}_l)\mathbf{H}^{-1}$. $\mathbf{q}_{act}(\mathbf{H}) = [q_{1-act}(H_1), q_{2-act}(H_2), \dots, q_{nn-act}(H_{nn})]^T$ = column vector of pressure/head-driven nodal demands, and \mathbf{q}_l = column vector of nodal leakage flow rates (assuming positive sign for node outflow). Actually, leakage occurs at pipe level and is just reported at the nodes as will be explained subsequently. The column vector $\mathbf{0}$ in the system [Eq. (1)] is related to the fact that the matrix \mathbf{A}_{nn} (by means of the vectors \mathbf{q}_{act} and \mathbf{q}_l) contains the pressure-driven demands and leakage flows.

For reasons of simplicity, while still preserving generality, elements such as pumps, valves, and other dissipation devices have not been considered in the simulation model (1). Furthermore, the single expression is used to define the head loss along the k th pipe in the network, regardless of the flow regime assumed and the head loss relationship used. Therefore, R_k = head loss coefficient that is a function of a pipe's roughness, diameter, and length, while n = exponent that takes into account the actual flow regime and the head loss relationship used (1.85 for the Hazen-Williams and 2 for the Darcy-Weisbach models).

In the system of Eq. (1), \mathbf{q}_{act} = column vector characterizing demand-pressure dependence whose elements are defined for the i th node of the network by the function $q_{i-act}(H_i)$ or $q_{i-act}(P_i)$ (see below). For $q_{i-act}(P_i)$, the following relationship will be used here (Wagner et al. 1988):

$$q_{i-act} = \begin{cases} q_{i-design} & \text{for } P_i > P_{i-ser} \\ q_{i-design} \left(\frac{P_i - P_{i-min}}{P_{i-ser} - P_{i-min}} \right)^{1/2} & \text{for } P_{i-min} \leq P_i \leq P_{i-ser} \\ 0 & \text{for } P_i < P_{i-min} \end{cases} \quad (2)$$

where P_{i-ser} = minimum service pressure required for supplying demand $q_{i-design}$ (those used for network design purposes, for example); and $[P_{i-ser}, P_{i-min}]$ = range of the intermediate working condition when the actual demand is given as q_{i-act} . For demands that are not pressure driven, Eq. (2) becomes $q_{i-act} = q_{i-design}$.

At the scale of individual pipes, the pressure-leakage relationship is defined in \mathbf{q}_l , a column vector whose elements are nodal leakages q_{i-leak} that is computed from the pipe leakage model q_{k-leak} . In order to avoid confusion among variables, the index i will be used for nodal-level variables and k for pipe-level variables. Thus, assuming a uniform distribution of leakage q_{k-leak} along pipe k , the background leakage model can be expressed as (Germanopoulos 1985; Germanopoulos and Jowitt 1989)

$$q_{k-leak} = \begin{cases} \beta_k l_k (P_k)^{\alpha_k} & \text{if } P_k > 0 \\ 0 & \text{if } P_k \leq 0 \end{cases} \quad (3)$$

where P_k = average pressure in the pipe computed as the mean of the pressure values at the end nodes i and j of the k th pipe; and l_k = length of that pipe. Variables α_k and β_k = two leakage model parameters (explained and discussed later in the text). The average pressure vector \mathbf{P}^{pipes} can be computed from the general topological matrix and nodal pressure as

$$\mathbf{P}^{pipes} = \frac{(|\bar{\mathbf{A}}_{pn}|[\mathbf{P}^{nodes} | \mathbf{P}_0^{nodes}])}{2} \quad (4)$$

where \mathbf{P}^{nodes} = pressure vector of unknown nodal heads; and \mathbf{P}_0^{nodes} = pressure vector of known nodal heads ($|\bar{\mathbf{A}}_{pn}|$ = absolute value of the topological matrix).

The allocation of leakage to the two end nodes can be performed in a number of ways. The simplest approach assumes that half of total leakage from the pipe element occurs at each of the end nodes. A more realistic approach, however, divides the total leakage in proportion with the magnitude of the two nodal pressures (Ainola et al. 2000). With either of these two approaches, the nodal leakage flow q_{i-leak} is computed as the sum of q_{k-leak} flows of all pipes connected to node i as follows:

$$q_{i-leak} = \sum_k \frac{1}{2} q_{k-leak} = \frac{1}{2} \sum_k \beta_k l_k (P_k)^{\alpha_k}$$

or

$$q_{i-leak} = \sum_k \frac{P_i}{P_i + P_j} q_{k-leak} = \frac{P_i}{2} \sum_k \beta_k l_k (P_k)^{\alpha_k - 1} \quad (5)$$

where $P_k = (P_i + P_j)/2$.

Thus, the elements of the vector \mathbf{q}_l can be computed from a topological matrices as follows:

$$\mathbf{q}_l = \left(\frac{1}{2} \text{ or } \frac{P_i}{2} \right) |\mathbf{A}_{np}| \begin{bmatrix} q_{1-leak} \\ 0 \\ q_{k-leak} \\ 0 \\ q_{np-leak} \end{bmatrix}$$

$$q_{k-leak} = \begin{cases} \beta_k l_k (P_k)^{\alpha_k} \text{ or } \beta_k l_k (P_k)^{\alpha_k - 1} & \text{if } P_k > 0 \\ 0 & \text{if } P_k \leq 0 \end{cases} \quad (6)$$

where $|\mathbf{A}_{np}|$ = absolute value of the matrix. Thus, the \mathbf{q}_l elements are from the matrix product involving topological matrix \mathbf{A}_{np} . The solution to the system of Eq. (1) for the pressure-driven demands defined in Eq. (2) was first given by Todini (2003). Here, the procedure is further expanded to account for pressure-driven leakage and to consider large networks. The procedure involves the initialization phase followed by the iteration phase as specified in the following equations.

Initialization Phase

$$\begin{aligned} \mathbf{\Lambda}_{pp}^{iter=0} &= \mathbf{I}_{pp} \\ \mathbf{\Lambda}_{nn}^{iter=0} &= \mathbf{I}_{nn} \\ \mathbf{H}^{iter=0} &= \mathbf{P}_{ser} + \mathbf{HL} \\ \mathbf{Q}^{iter=0} &= (\mathbf{R}_{pp})^{-1} \end{aligned} \quad (7a)$$

where \mathbf{I}_{nn} and \mathbf{I}_{pp} = identity matrices; $\mathbf{\Lambda}_{nn}$ and $\mathbf{\Lambda}_{pp}$ = diagonal matrices of over-relaxation coefficients for nodal heads and pipe flow updating; \mathbf{R}_{pp} = vector whose elements are R_k ; \mathbf{HL} = vector of nodal elevations; \mathbf{P}_{ser} = vector whose elements are P_{i-ser} . The initialization part of the algorithm shown in Eq. (7a) ensures that flows $\mathbf{Q}^{iter=0}$ make $\mathbf{D}_{pp} = \mathbf{I}_{pp}$ for $iter=0$.

Iteration Phase

$$\mathbf{A}^{\text{iter}} = \mathbf{A}_{\text{np}}(\mathbf{D}_{\text{pp}}^{\text{iter}})^{-1}\mathbf{A}_{\text{pn}} - (\mathbf{D}_{\text{nn}}^{\text{iter}} + \mathbf{DL}_{\text{nn}}^{\text{iter}})$$

$$\mathbf{F}^{\text{iter}} = [\mathbf{A}_{\text{np}}\mathbf{Q}^{\text{iter}} - (\mathbf{q}_{\text{act}}^{\text{iter}} + \mathbf{q}_l^{\text{iter}})] - \mathbf{A}_{\text{np}}(\mathbf{D}_{\text{pp}}^{\text{iter}})^{-1}(\mathbf{A}_{\text{p0}}\mathbf{H}_0 + \mathbf{A}_{\text{pp}}^{\text{iter}}\mathbf{Q}^{\text{iter}}) - (\mathbf{D}_{\text{nn}}^{\text{iter}} + \mathbf{DL}_{\text{nn}}^{\text{iter}})\mathbf{H}^{\text{iter}}$$

$$\mathbf{H}^{\text{iter}+1} = (\mathbf{A}^{\text{iter}})^{-1}\mathbf{F}^{\text{iter}}$$

$$\mathbf{Q}^{\text{iter}+1} = \mathbf{Q}^{\text{iter}} - (\mathbf{D}_{\text{pp}}^{\text{iter}})^{-1}(\mathbf{A}_{\text{pp}}^{\text{iter}}\mathbf{Q}^{\text{iter}} + \mathbf{A}_{\text{pn}}\mathbf{H}^{\text{iter}+1} + \mathbf{A}_{\text{p0}}\mathbf{H}_0)$$

$$\mathbf{H}^{\text{iter}+1} = \mathbf{A}_{\text{nn}}^{\text{iter}}(\mathbf{H}^{\text{iter}+1} - \mathbf{H}^{\text{iter}}) + \mathbf{H}^{\text{iter}}$$

$$\mathbf{Q}^{\text{iter}+1} = \mathbf{A}_{\text{pp}}^{\text{iter}}(\mathbf{Q}^{\text{iter}+1} - \mathbf{Q}^{\text{iter}}) + \mathbf{Q}^{\text{iter}} \quad (7b)$$

In the iterative part of the algorithm, \mathbf{D}_{nn} , \mathbf{DL}_{nn} , and \mathbf{D}_{pp} are diagonal matrices whose elements denote derivatives of \mathbf{q}_{act} , \mathbf{q}_l elements and $R_k|Q_k|^{n-1}Q_k$ with respect to nodal pressure, pipe pressure, and pipe flow, respectively. For example, $\mathbf{D}_{\text{nn}}=(n_n, n_n)$ diagonal matrix given as

$$\mathbf{D}_{\text{nn}}(i,i) = \begin{cases} 0 & \text{for } P_i > P_{i-\text{ser}} \\ \frac{q_{i-\text{design}}}{2} \frac{(P_i - P_{i-\text{min}})^{-1/2}}{(P_{i-\text{ser}} - P_{i-\text{min}})^{1/2}} & \text{for } P_{i-\text{min}} \leq P_i \leq P_{i-\text{ser}} \\ 0 & \text{for } P_i < P_{i-\text{min}} \end{cases} \quad (8)$$

and \mathbf{DL}_{nn} represents a (n_n, n_n) diagonal matrix whose elements can be calculated from the derivatives of $q_{k-\text{leak}}$ with respect to P_k [see Eq. (5)]. Similarly to matrix \mathbf{q}_l in Eq. (6), elements of matrix $\mathbf{DL}_{\text{nn}}(i,i)$ can be obtained as follows:

$$\mathbf{DL}_{\text{nn}}(i,i) = \left(\frac{1}{2} \text{ or } \frac{P_i}{2} \right) \left| \mathbf{A}_{\text{np}} \right| \begin{bmatrix} \frac{dq_1}{dP_1} \\ 0 \\ \frac{dq_k}{dP_k} \\ 0 \\ \frac{dq_{\text{np}}}{dP_{\text{np}}} \end{bmatrix}$$

$$\frac{dq_k}{dP_k} = \alpha_k \beta_k I_k (P_k)^{\alpha_k-1} \text{ or } \frac{dq_k}{dP_k} = (\alpha_k - 1) \beta_k I_k (P_k)^{\alpha_k-2} \quad \text{if } P_k > 0$$

$$\frac{dq_k}{dP_k} = 0 \quad \text{if } P_k \leq 0 \quad (9)$$

Moreover, the diagonal elements of both \mathbf{A} matrices are assumed equal to λ^{iter} (a real number in the $[0,1]$ range) that works as a step size, or over-relaxation coefficient, for updating nodal heads and pipe flow rates across iterations. It is worth noting that $\lambda^{\text{iter}=0}$ is set to 1, meaning that the relaxation coefficient is not used initially, but its adaptation to the error surface (during the iterative search for the solution) is invoked if required to improve convergence behavior. Here, the value of λ^{iter} is driven by the mean of squared errors or by the maximum errors in the mass and energy balance equations while performing the iterative search. When any of these errors decreases, the value of λ^{iter} increases by a factor of 5 and when any of these errors increases, the value of λ^{iter} is reduced by a factor of 10. If, during the iterative search, λ^{iter} becomes equal to or less than the error tolerance level (e.g.,

10^{-7}) or mean of squared errors (e.g., 10^{-7}), the search process is stopped because convergence has been reached. Experiments carried out by the authors have shown that model runs, described below, performed without the relaxation coefficient procedure can have serious convergence problems.

Furthermore, the initialization of flows used here makes the matrix \mathbf{D}_{pp} (initialized to \mathbf{I}_{pp}) well conditioned, which is particularly useful for large networks. The maximum number of iterations is also used as a further threshold control.

Finally, assuming separate expressions for background leakage, $q_{k-\text{background}}$, and burst losses, $q_{k-\text{burst}}$, the total leakage $q_{k-\text{leak}}$ along the pipe k th can be expressed using:

1. The classical formulas of orifice flow for bursts (exponent equal to 0.5); and
2. the Germanopoulos (1985) expression for background losses with different meaning assigned to its constants

$$\begin{cases} q_{k-\text{leak}} = \beta_k I_k (P_k)^{\alpha_k} + C_k (P_k)^{0.5} & \text{if } P_k > 0 \\ q_{k-\text{leak}} = 0 & \text{if } P_k \leq 0 \end{cases} \quad (10)$$

where α_k and β_k =two parameters of the leakage flow model related to the background losses only, and C_k =coefficient dependent on the sum of outflow coefficients related to bursts along the pipe. Therefore, Eqs. (5) can be rewritten as follows:

$$q_{i-\text{leak}} = \sum_k \frac{1}{2} q_{k-\text{leak}} = \frac{1}{2} \sum_k \beta_k I_k (P_k)^{\alpha_k} + C_k (P_k)^{0.5}$$

or

$$q_{i-\text{leak}} = \sum_k \frac{P_i}{P_i + P_j} q_{k-\text{leak}} = \frac{P_i}{2} \sum_k \beta_k I_k (P_k)^{\alpha_k-1} + C_k (P_k)^{-0.5} \quad (11)$$

Note that Eqs. (7) and (9) can be easily modified by following the above reasoning.

Leakage Model Parameters (α and β)

Water distribution system losses may be classified as being due to: Background losses (from joints, fittings, and small cracks); reported bursts; and unreported bursts (Lambert 1994).

The main explanation for growing water loss (either due to bursts or small cracks) is the general deterioration of water mains, joints, and service connections. Pipe degradation (pipe parameter β) has commonly been studied as a steady monotonic process that is modified by time-varying "noise" (Kleiner and Rajani 2002). Pipe age, diameter, and material have been identified as primary variables influencing the monotonic increase in the burst rate over a number of years. The majority of statistical methods consider pipe age as the most crucial variable describing the increase in pipe failure rates over time (Shamir and Howard 1979; Kleiner and Rajani 2001). Furthermore, Walski and Pelliccia (1982) found diameter to be a key factor, with the failure rate of smaller diameter pipes being higher than those experienced by larger ones. Studies of common metallic pipe (e.g., cast iron, ductile iron, etc.) behavior have been conducted to establish the influence of pipe material on failure rates (Kleiner and Rajani 2002; Kettler and Goulter 1985). Moreover, age, material, and diameter are usually the only, if any, information available to many municipalities and water companies. Recently, Berardi et al. (2005) demonstrated the dependence of pipe bursts on pipe length, age, and diameter using real data from UK water companies.

The value of the leakage parameter α in Eq. (5) can be described using the fixed and variable area discharge approach proposed by May (1994). In fact, May originally suggested a two-component model, burst losses through a constant area hole ($\alpha=0.5$) and background losses through an area that changes linearly with pressure ($\alpha=1+0.5=1.5$). Thus, α of the leakage model [Eq. (5)] depends on the balance between the burst ($\alpha=0.5$) and background ($\alpha>0.5$) leakage flows and can be determined by means of model calibration and/or component analysis. For example, Jowitt and Xu (1990) and Vairavamorthy and Lumbers (1998) obtained the value of $\alpha=1.18$ from field data. Later, Lambert (2001) inferred a range of α values ranging from 0.50 to as high as 2.50, depending on the mixture of leaks and the dominant type of leaks (simple holes: $\alpha=0.5$; longitudinal split that opens in one dimension: As in May (1994), i.e., $\alpha=1.5$; linear-radial opening: $\alpha=2.0$ – 2.5). Plastic pipes exhibit higher α values because of their propensity to have longitudinal splits. Interestingly, Lambert (2001) reported α values around 1.5 regardless of the pipe material. However, it is currently held that rigid pipes such as those comprised of metal are generally characterized by lower values of α .

Based on the above discussion, the following functional relationships can be postulated for α and β

$$\alpha_k = \alpha_k \left(\frac{d_k}{s_k}, m_k \right) \quad 1 \leq k \leq n_p$$

$$\beta_k = \beta_k(\text{age}_k, d_k, s_k, m_k, \text{pr}_k, \dots) \quad 1 \leq k \leq n_p \quad (12)$$

where m =the pipe material; pr =number of properties supplied (or connections on the main); and s =pipe wall thickness. From Eq. (12) that β depends, in general, on both pipe characteristics and various external factors (e.g., environmental conditions, traffic loading, external stress and corrosion, etc.). In contrast, α is a function of pipe characteristics only (material m and rigidity d/s).

Clearly, the change in β over the years is related to average pressure (Lambert 2001). From the standpoint of functional dependency, this is accounted for by the pipe age variable while, from a physical perspective, pressure generates a fatigue effect (i.e., enhancing deterioration) similar to that of traffic loading. Thus, for a specific system, escalation in the leakage rate can be described by pipe age.

Similar to pipe breaks (Shamir and Howard 1979), an exponential formulation can be used for leakage proliferation (Walski 1987). Thus, $\beta(\text{age})$ exponentially increases at a rate whose coefficient in the function argument is dependent on the pressure regime since the rate of system deterioration is influenced by pressure management (Lambert 2001). The value of this coefficient for the leakage increase rate, as reported in Walski (1987), can be assumed close to zero in systems where utilities routinely conduct leak repair activities, while the coefficient of pipe break growth is a reasonable estimate for a utility without an ongoing leak detection program.

Finally, β is more closely related to the number of leaks (or leakage area) per unit of pipe length while α is more strongly related to the type of leakage (therefore to the hydraulics of leakage) as governed by pipe material (Lambert 2001).

Case Studies

The objective of the case studies is neither to perform a water balance nor to calibrate leakage model parameters, but to demon-

strate the effectiveness of the proposed simulation model (coupling pressure-driven nodal demands and pipe leakage) in the context of both small and large networks. The two case studies, whose characteristics are derived from real systems (named “Network A” and “Network B”, respectively), serve to:

- Show that the new modeling approach provides more realistic results when applied to a classical optimal network design problem (base case for comparison). For this purpose, the hypothesis of leakage flow rates proportional to nodal demands will be discussed.
- Test the new simulation model from a numerical standpoint, by analyzing convergence through some performance indicators.

To demonstrate that the new modeling approach provides more realistic results than the demand-driven analysis, the two networks were optimized to obtain the least-cost design for each of them [see for example, Savic and Walters (1997) for the formulation of the optimization problem] and the solutions were tested using the pressure-driven approach. The layout of the smaller network (“Network A”), whose characteristics were derived from a real Italian system, is depicted in Fig. 1 with corresponding data provided in Tables 1–3. Pipe diameters in Table 2 have been determined by minimizing the total design cost subject to a minimum pressure \mathbf{P}_{ser} (equal to 10 m for all the nodes) constraint for supplying the prescribed demand $\mathbf{q}_{\text{design}}$ (base case). Based on common practice where leakage is assumed to represent a percentage of nodal demand (e.g., 25% in Italy), the actual required demand was adopted for the design study as $\mathbf{q}_{\text{demand}} = \mathbf{q}_{\text{design}}/1.25$. The following relationship was used for the pipe roughness calculation

$$R_k = \frac{8.57 \times 10^{-4} (1 + 2\gamma/\sqrt{d_k})^2}{d_k^5} l_k \quad k = 1, 2, \dots, n_p \quad (13)$$

where R_k =pipe resistance coefficient; d_k =pipe diameter; l_k =pipe length; and $\gamma=0.12$ =Bazin friction factor. Note that the Bazin formula is commonly used in Italy and the previous study was undertaken using this expression. For the pressure-driven demand model, the value $\mathbf{P}_{\text{min}}=0$ is applied at all nodes while Eq. (3) is used for the leakage model.

The larger size network (“Network B,” Fig. 2) was derived from a real UK system. The network consists of 1,991 pipes, 1,461 internal nodes, and five reservoirs (head varying from 40 to 50 m). The diameters used for optimal pipe sizing are those in Table 1 and some statistics of the network are provided in Table 4. The least-cost design was performed by minimizing the total design cost subject to a minimum pressure \mathbf{P}_{ser} (equal to 20 m for all the nodes) constraint for supplying the design demand $\mathbf{q}_{\text{design}}$ (using $\mathbf{q}_{\text{demand}} = \mathbf{q}_{\text{design}}/1.25$). Finally, the value \mathbf{P}_{min} was set equal to 10 m for all the nodes.

Network Design with Leakage Considerations

Network designs obtained from demand-driven analysis assume leakage proportional to nodal demand at each node, but independent of network nodal pressure, leading to unrealistic nodal leakage estimates. For example, two obvious and significant drawbacks of the unrealistic assumption of a constant leakage percentage normally employed with demand-driven simulation (when combined with optimization for network design) are:

- The resultant low leakage flows for nodes experiencing low

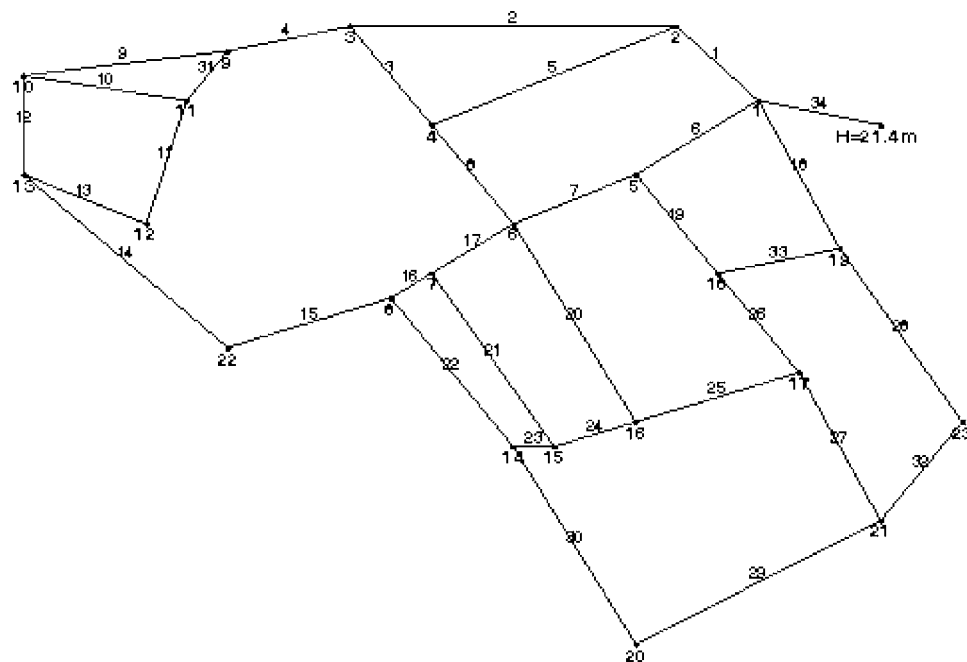


Fig. 1. Layout of "Network A"

demand, even if they experience high nodal pressure (e.g., are close to a tank).

- The fact that two nodes having equal demand will have equal leakage flow rates associated with them despite their actual hydraulic positions in the network (pressure levels) related to elevations, tank and pump locations, etc.

In order to analyze the effects of the constant-percent leakage assumption, the first step was to calibrate β of the leakage model for both networks. To perform this task, the value of α was set to 1.2 and the simulations were performed using q_{demand} for both networks, forcing the total leakage flow rate to 25% of q_{demand} . The results obtained were $\beta = 1.0632 \times 10^{-7}$ and $\beta = 2.0748 \times 10^{-8}$ for networks "A" and "B," respectively. The first observation is that, because of the differing total pipe length and average network pressure, β differs by one order of magnitude between the networks. This demonstrates that a simulation model taking into account the real β is useful even if only used for design purposes, because the value for leakage flow rates should be re-

lated to the total length, pressure, predicted deterioration, and other factors of the system rather than a constant value (e.g., 25% used here).

Therefore, the real-losses component of the water balance and/or analysis of night flows based on district metering data (Lambert and Hirner 2000) can be used for determining comprehensive or zonal values for the leakage flow model parameters in order to plan rehabilitation/expansion of the network. β may be seen as a pipe parameter that requires calibration, similar to roughness, using as prior information β_0 from water balance or other analyses. For a new network, or a network extension, the concept of unavoidable average real losses and infrastructure leakage index [see Lambert and Hirner (2000)], can be used for design purposes to establish a value for β instead of using a constant-percent coefficient.

Furthermore, Figs. 3–6 show the pressure and leakage flow differences for both systems, as computed using the two approaches, demand-driven and pressure-driven simulations. Figs. 3 and 5 report the percentage difference in pressure at each node in the network computed with respect to the nodal pressures of the base design case, while Figs. 4 and 6 show the nodal leakage flow rates, normalized to the total required network demand, used during the design phase compared to those computed with the pressure-driven simulation. Figs. 3 and 5 demonstrate that the majority of the nodes are characterized by a positive pressure difference. This means that the realistic simulation of leakage flow results in a generally higher pressure status than the demand-driven simulation using a constant-percent nodal leakage. The general rise in network pressures is explained by the fact that overall flow throughout pipes has decreased due to greater leakage at nodes with high pressure (e.g., close to tanks).

Figs. 4 and 6 present a different outcome of nodal leakage flow computation (referred to total network demand) between the two simulation approaches. Results for "Network A" illustrate how the nodes closest to the tank are characterized by greater leakage flows (pressure-driven simulation), while the most downstream nodes experience lower leakage. More interesting is the situation

Table 1. Diameters Used for Pipe Sizing of Networks "A" and "B"

d (m)	R/l (s^2/m^6)
0.100	265.147
0.164	18.565
0.184	9.882
0.204	5.629
0.229	3.068
0.258	1.639
0.290	0.867
0.327	0.460
0.368	0.247
0.500	0.049
0.750	0.006
1.000	0.001

Table 2. “Network A” Pipe Data

Pipe number	Start node	End node	l_k (m)	d_k (m)
1	1	2	348.5	0.327
2	2	3	955.7	0.290
3	3	4	483	0.100
4	3	9	400.7	0.290
5	2	4	791.9	0.100
6	1	5	404.4	0.368
7	5	6	390.6	0.327
8	6	4	482.3	0.100
9	9	10	934.4	0.100
10	11	10	431.3	0.184
11	11	12	513.1	0.100
12	10	13	428.4	0.184
13	12	13	419	0.100
14	22	13	1,023.1	0.100
15	8	22	455.1	0.164
16	7	8	182.6	0.290
17	6	7	221.3	0.290
18	1	19	583.9	0.164
19	5	18	452	0.229
20	6	16	794.7	0.100
21	7	15	717.7	0.100
22	8	14	655.6	0.258
23	15	14	165.5	0.100
24	16	15	252.1	0.100
25	17	16	331.5	0.100
26	18	17	500	0.204
27	17	21	579.9	0.164
28	19	23	842.8	0.100
29	21	20	792.6	0.100
30	20	14	846.3	0.184
31	9	11	164	0.258
32	23	21	427.9	0.100
33	19	18	379.2	0.100
34	24	1	158.2	0.368

depicted in Fig. 6 related to “Network B.” Here, the nodes have been sorted in ascending order according to assigned flow rates (from the design phase) in order to better visualize the results. Fig. 6 gives further evidence of the unrealistic assumption of constant-percent leakage used for design. In fact, there are nodes that have zero, or near zero, demand (and consequently low assumed leakage flow rate), while some (see, for example, the maximum value of 0.5% of the total network demand) experience a high flow rate as a consequence of high demand. The pressure-driven simulation approach shows more equally distributed nodal leakage flows (around a value close to 0.02%), which is a more realistic representation of leakage in this case.

Convergence and Robustness of the Simulation Model

Here, the proposed simulation model with pressure-driven demand and leakage is tested for convergence in a steady-state mode. In order to carry out the test, 1,000 simulations were per-

Table 3. “Network A” Node Data

Node ID	$q_{i\text{-design}}$ (l/s)	HL_i (m)	P_i (m)
1	10.863	6.4	26.90
2	17.034	7	24.81
3	14.947	6	21.30
4	14.280	8.4	17.22
5	10.133	7.4	23.54
6	15.35	9	20.10
7	9.114	9.1	18.91
8	10.510	9.5	17.90
9	12.182	8.4	17.85
10	14.579	10.5	12.66
11	9.007	9.6	16.23
12	7.575	11.7	10.12
13	15.200	12.3	10.03
14	13.550	10.6	15.41
15	9.226	10.1	14.00
16	11.200	9.5	14.36
17	11.469	10.2	15.30
18	10.818	9.6	18.83
19	14.675	9.1	19.35
20	13.318	13.9	10.01
21	14.631	11.1	11.48
22	12.012	11.4	14.00
23	10.326	10	10.45
24		15	$H_{01}=21.4+15$

formed for both networks simultaneously varying the following parameters:

- The roughness values for each pipe (R_k).
 - The values of each pipe leakage coefficient (β_k).
 - The value of α applied over the entire network.
- The simulations were performed using the values of the above parameters sampled as follows:
- The roughness values for each pipe (R_k) were sampled uniformly from the range of $\pm 50\%$ around those related to the optimal values obtained in the network design process (base case).
 - The values of each pipe leakage coefficient (β_k) were sampled from the range $[1 \times 10^{-8}, 1 \times 10^{-6}]$ and $[2 \times 10^{-9}, 2 \times 10^{-7}]$ for Networks “A” and “B,” respectively. The upper and lower boundaries of the sampling range have been selected to be an order of magnitude smaller/greater than β calibrated in previously described exercise, assuming a water loss of 25%.
 - The value of α applied over the entire network was sampled from the range $[0.5, 2.5]$.

Sampling was performed here using Monte Carlo methodology and, specifically, the Latin hypercube technique (McKay et al. 1979) was used as the variance reduction method for limiting the number of samples required for more extensive coverage of the sample space. As indicated, convergence was assumed when λ^{iter} became less than 10^{-7} or the mean of squared errors was less than or equal to 10^{-7} . A notebook computer with a Pentium Intel M 1.10 GHz processor was used for simulations.

Furthermore, the simulation model was tested without using the over-relaxation parameter λ^{iter} on Network “B” (the largest one) in order to assess its effectiveness.

Tables 5 and 6 report selected hydraulic parameters for both networks, including flow rates, average network pressure (P_{avg}),

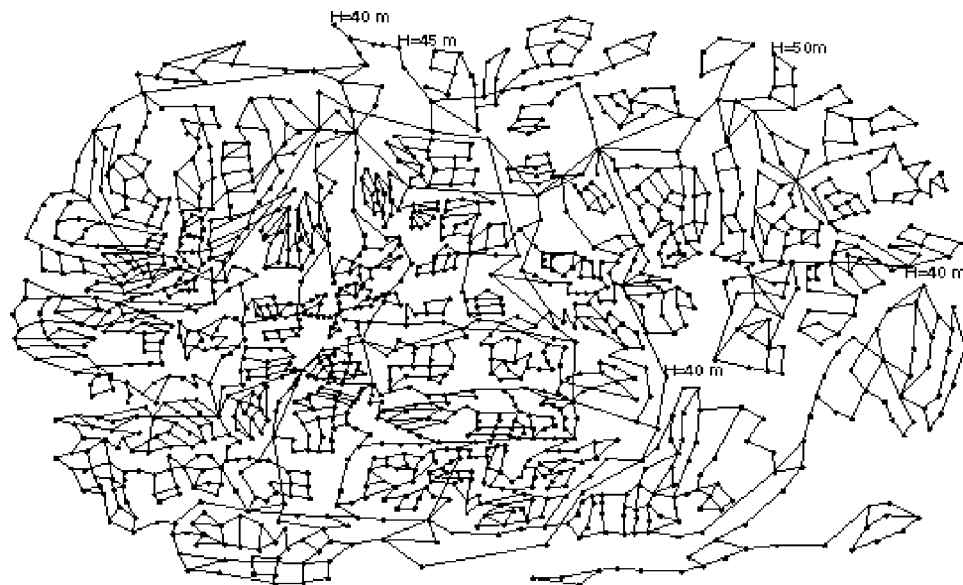


Fig. 2. Layout of "Network B"

and number of critical nodes, all revealing the extent of tested conditions.

The first row of Tables 7 and 8 reports the average statistics of the 1,000 simulations considering both the maximum energy/mass balance errors (first and second columns), the mean energy/mass balance errors (third and fourth columns), the average number of iterations (fifth column) and the average CPU time required for each simulation (sixth column). The second row indicates the worst results of the above statistical parameters. Furthermore, Table 8 reports the same statistics (fifth and sixth columns) achieved without using the over-relaxation parameter λ^{iter} . They refer to simulations performed on "Network B" using the same parameters (R_k , β_k , α) as in the runs with the over-relaxation parameter (λ^{iter}) being used. The statistics were computed on 960 simulations (instead of the 1,000 runs performed) to avoid bias

Table 4. Range of Some Parameters of the "Network B"

	l_k (m)	$q_{i\text{-design}}$ (l/s)	R_k (s^2/m^5)
Total/mean	486,927	3183.4	6,155.6
Minimum	1	0	0.0013
Maximum	2,530	63	530,293.3

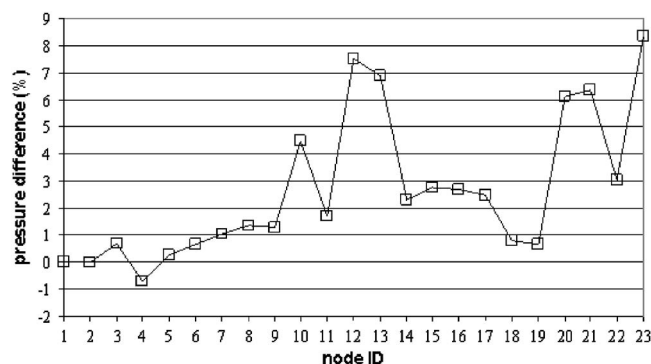


Fig. 3. Nodal pressure difference (in percentage of the nodal design pressure) between the two simulation approaches ("Network A")

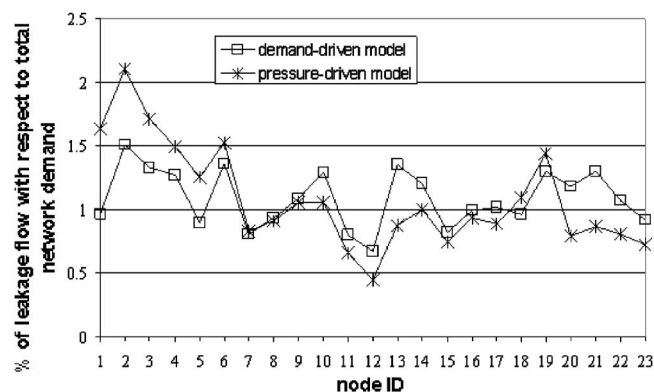


Fig. 4. Percentage (referring to total network demand) of nodal leakage flow of the two simulation approaches ("Network A")

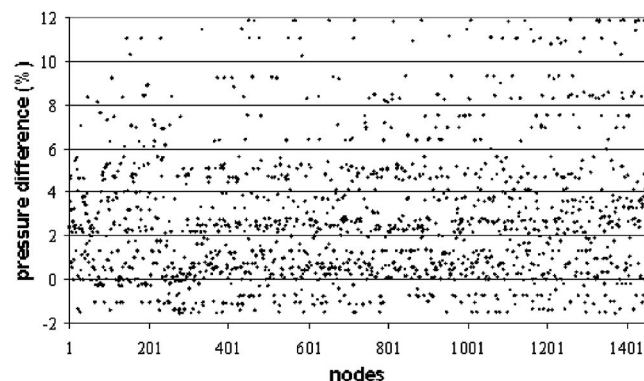


Fig. 5. Nodal pressure difference (in percentage of the nodal pressure of design) between the two simulation approaches ("Network B")

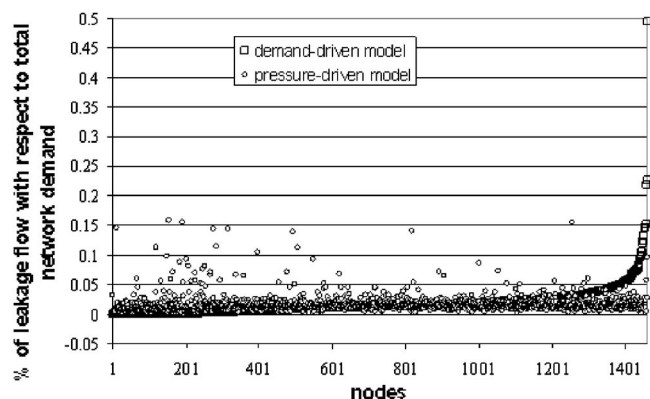


Fig. 6. Percentage (referring to total network demand) of nodal leakage flow of the two simulation approaches (“Network B”)

Table 5. Minimum/Maximum Value of Some Useful Parameters during Leakage-Driven Simulations. N_{CR} Is the Number of Critical Nodes ($P_i < P_{i-ser}$).

“Network A”	q_l/q_{demand}	N_{CR}	q_{act} (m^3/s)	q_l (m^3/s)	P_{avg} (m)
Minimum among the 1,000 simulations	0.1501	0	0.1005	0.0339	2.78
Average among the 1,000 simulations	1.1833	13	0.1803	0.2669	9.61
Maximum among the 1,000 simulations	3.4701	22	0.2256	0.7829	19.81

Note: q_{act} and q_l here mean total network supplied demand and leakage outflow, respectively.

Table 6. Minimum/Maximum Value of Some Useful Parameters during Leakage-Driven Simulations. N_{CR} Is the Number of Critical Nodes ($P_i < P_{i-ser}$).

“Network B”	q_l/q_{demand}	N_{CR}	q_{act} (m^3/s)	q_l (m^3/s)	P_{avg} (m)
Minimum among the 1,000 simulations	0.1110	0	0.1381	0.2826	6.70
Average among the 1,000 simulations	2.0197	708	1.5709	5.1436	19.18
Maximum among the 1,000 simulations	5.5924	1,225	2.5467	14.2421	33.62

Note: q_{act} and q_l here mean total network supplied demand and leakage outflow, respectively.

Table 7. Statistics of Leakage-Driven Simulations

	Maximum error		Mean error		Iteration number	CPU time (s)
	Energy balance (m)	Mass balance (m^3/s)	Energy balance (m)	Mass balance (m^3/s)		
“Network A”						
Average among the 1,000 simulations	4.50×10^{-4}	1.63×10^{-4}	3.82×10^{-5}	2.49×10^{-5}	9.84	0.012
Worst among the 1,000 simulations	2.24×10^{-3}	1.44×10^{-3}	2.11×10^{-4}	1.64×10^{-4}	25	0.047

Table 8. Statistics of Leakage-Driven Simulations

		Maximum error		Mean error		Iteration number	CPU time (s)
		Energy balance (m)	Mass balance (m^3/s)	Energy balance (m)	Mass balance (m^3/s)		
“Network B”							
Using λ^{iter}	Average among the 1,000 simulations	5.32×10^{-3}	8.91×10^{-5}	4.45×10^{-6}	1.54×10^{-7}	21.09	1.82
	Worst among the 1,000 simulations	1.84×10^{-2}	6.32×10^{-3}	2.89×10^{-5}	4.81×10^{-6}	51	4.53
Without using λ^{iter}	Average among the 960 simulations	5.34×10^{-3}	9.10×10^{-5}	4.01×10^{-6}	9.36×10^{-8}	21.18	2.07
	Worst among the 960 simulations	1.85×10^{-2}	1.62×10^{-2}	2.23×10^{-5}	1.11×10^{-5}	44	5.16

caused by runs experiencing serious convergence problems (10 simulations) or the complete lack of convergence (30 simulations).

The statistics of “Network A” compared with those of “Network B” (see the maximum errors that are not biased by the network size) prove that by increasing the network size (i.e., number of variables), the algorithm performance does not deteriorate significantly. Furthermore, the statistics in Table 8 for “Network B” show that the achieved maximum errors (about 6 l/s for flow and about 1.8 cm for pressure) and the average errors (about 0.005 l/s for flow and about 0.03 mm for pressure) of the worst simulation (among 1,000) are, for all practical purposes, within the acceptable range. The average number of iterations needed for convergence was about 21, while the average run time was about 1.8 sec. The maximum number of iterations was 51 and the maximum run time for a single simulation was about 4.5 sec.

Furthermore, Fig. 7 reinforces the evidence of the algorithm’s robustness, showing the number of iterations for each simulation. They are clustered around the values of about 20, while for only about 3% of simulations more than 30 iterations were required.

The beneficial influence of the over-relaxation parameter λ^{iter} on convergence of the algorithm was proven experimentally by eliminating problems experienced in 4% of runs (a very slow convergence for 10 and absence of convergence for 30, out of 1,000 runs). Furthermore, the use of the over-relaxation parameter improves the algorithm run times, but the comparison of the statistics shows only a slight improvement in the average number of algorithm iterations when using λ^{iter} , while the CPU time decreased by approximately 10%. The observation that the single algorithm iteration generally requires less CPU time when using the over-relaxation parameter could be explained by the fact that the solution of the linear system [based on vector \mathbf{F} and matrix \mathbf{A} in the algorithm (7b)] requires fewer iterations.

In summary, the over-relaxation parameter has proven to be effective for providing robustness to the simulation model. This is explained by the fact that the over-relaxation parameter guides the search for \mathbf{H} and \mathbf{Q} vectors to the most promising regions of the search space. However, the selected initialization [Eq. (7a)] influences the algorithm convergence; therefore, it is more important for larger networks because of the increase in dimensionality that makes the error surface more complex during the iterative search. Finally, as a secondary effect, the over-relaxation parameter

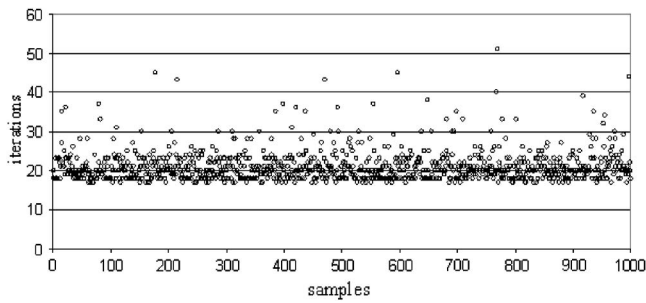


Fig. 7. Number of iterations for convergence for each simulation ("Network B")

seems to generally increase convergence of the linear system solution inside each algorithm iteration [Eq. (7b)].

Conclusions

A new hydraulic simulation model capable of the simultaneous quantification of pressure-driven demands and leakage is presented. The steady-state network model was developed by fully integrating system demands (both customer demands and leaks) at the pipe level into the hydraulic model. The importance of an improved leakage model for more realistic network simulation was demonstrated using pipe network design solutions. The comparison of leakage flows for networks designed using demand-driven simulation under the assumption of a constant-percent nodal leakage, shows that the realistic simulation of leakage flow results in generally higher pressures across a network than for the demand-driven simulation. The general rise in network pressures for the specific networks (elevations, topology, nodal demands, etc.) is explained by the decrease in overall flow throughout pipes due to greater leakage at nodes with high pressure (e.g., close to tanks). From a numerical standpoint, the algorithm convergence behavior was tested using one small and one large network derived from two real systems. All the observed convergence/error statistics reinforce the notion that the pressure-driven demand and leakage simulation model developed and presented herein is robust.

Acknowledgments

The writers wish to thank the associate editor and reviewers for their thorough and insightful review of the manuscript. The reviews have proven to be particularly important for improving the quality of this article.

Notation

The following symbols are used in this paper:

- \mathbf{A} = temporary matrix used in simulation model algorithm;
- \mathbf{A}_{nn} = diagonal matrix whose elements are from the scalar product $-(\mathbf{q}_{act} + \mathbf{q}_l)\mathbf{H}^{-1}$;
- $\bar{\mathbf{A}}_{pn}$ = general topological matrix;
- $\mathbf{A}_{pn}, \mathbf{A}_{np}$ = topological incidence submatrices;
- \mathbf{A}_{pp} = diagonal matrix whose elements are $R_k|Q_k|^{n-1}$;

- age = age of the pipe in the statistical model of pipe failure;
- C_k = coefficient for burst leakage model for k th pipe;
- \mathbf{D}_{nn} = diagonal matrices whose elements are derivatives of \mathbf{q}_{act} elements;
- \mathbf{D}_{pp} = diagonal matrices whose elements are derivatives of $R_k|Q_k|^{n-1}Q_k$;
- \mathbf{DL}_{nn} = diagonal matrices whose elements are derivatives of \mathbf{q}_l elements;
- d/d_k = diameter of the k th pipe;
- \mathbf{F} = temporary matrix used in Todini's algorithm;
- \mathbf{H} = vector of total network heads;
- \mathbf{H}_0 = vector of total fixed (i.e., known) network heads;
- $\mathbf{I}_{nn}, \mathbf{I}_{pp}$ = identity matrices;
- i = matrix index for nodes;
- iter = iteration counter;
- k = matrix index for pipes;
- l/l_k = length of the k th network pipe;
- m_k = material of k th pipe;
- n = head loss equation exponent and submatrix index;
- n_n = total number of network nodes;
- n_0 = total number of known heads;
- n_p = total number of network pipes;
- P_{avg} = average pressure of the network;
- $\mathbf{P}/\mathbf{P}^{nodes}$ = vector of nodal pressure heads;
- \mathbf{P}_0^{nodes} = vector of known nodal pressure heads;
- \mathbf{P}^{pipes} = vector of average pressure in pipes whose components are P_k ;
- \mathbf{P}_{min} = vector of minimum pressures at which demand supplied is equal to zero;
- \mathbf{P}_{ser} = vector of minimum pressures required for supplying the demand \mathbf{q}_{design} ;
- pr_k = number of properties supplied along the k th pipe;
- \mathbf{Q} = vector of pipe flows;
- \mathbf{q}_{act} = vector of (actually) supplied nodal demands;
- \mathbf{q}_{demand} = vector of actual required demand assuming 25% of leakages ($\mathbf{q}_{demand} = \mathbf{q}_{design}/1.25$);
- \mathbf{q}_{design} = vector of nodal demands used for pipe sizing;
- \mathbf{q}_l = vector of nodal flow rates from leakage outflow model at pipe level;
- q_{i-leak} = leakage flow rate in i th node;
- q_{k-leak} = leakage flow rate in k th pipe;
- $q_{k-bursts}$ = burst component of leakage flow rate in k th pipe;
- $q_{k-background}$ = background losses component of leakage flow rate in k th pipe;
- R_k = pipe hydraulic roughness;
- \mathbf{R}_{pp} = vector whose elements are pipe hydraulic roughness;
- s_k = thickness of the k th pipe;
- α_k, β_k = coefficients of the leakage model for k th pipe;
- γ = Bazin's friction factor;
- $\Lambda_{nn}, \Lambda_{pp}$ = diagonal matrices of over-relaxation coefficients; and
- λ^{iter} = step size or over-relaxation coefficient at $iter$ th iteration.

Operators and Acronyms

- $()^T$ = vector/matrix transpose operator.

References

- Ackley, J. R. L., Tanyimboh, T. T., Tahar, B., and Templeman, A. B. (2001). "Head-driven analysis of water distribution systems." *Proc., Computer and Control in Water Industry (CCWI), Water Software Systems: Theory and Applications*, B. Ulanicki, ed., Vol. 1, Research Studies Press, England, 183–192.
- Ainola, L., Koppel, T., Tiiter, T., and Vassiljev, A. (2000). "Water network model calibration based on grouping pipes with similar leakage and roughness estimates." *Proc., Joint Conf. on Water Resource Engineering and Water Resource Planning and Management (EWRI) (CD-ROM)*, <http://cedb.asce.org>.
- Almandoz, J., Cabrera, E. M., Arregui, F., Cabrera, E., Jr., and Cobacho, R. (2005). "Leakage assessment through water distribution network simulation." *J. Water Resour. Plann. Manage.*, 131(6), 458–466.
- Berardi, L., Savic, D. A., and Giustolisi, O. (2005). "Investigation of burst-prediction formulas for water distribution systems by evolutionary computing." *Proc., Computer and Control in Water Industry (CCWI)*, Vol. 2, 275–280.
- Chandapillai, J. (1991). "Realistic simulation of water distribution system." *J. Transp. Eng.*, 117(2), 258–263.
- Colombo, A. F., and Karney, B. W. (2002). "Energy and costs of leaky pipes: Toward a comprehensive picture." *J. Water Resour. Plann. Manage.*, 128(6), 441–450.
- Germanopoulos, G. (1985). "A technical note on the inclusion of pressure dependent demand and leakage terms in water supply network models." *Civ. Eng. Syst.*, 2, 171–179.
- Germanopoulos, G., and Jowitt, P. W. (1989). "Leakage reduction by excessive pressure minimization in a water supply network." *Proc. Inst. Civ. Eng., Part 2. Res. Theory*, 87, 195–214.
- Gupta, R., and Bhave, P. R. (1996). "Comparison of methods for predicting deficient-network performance." *J. Water Resour. Plann. Manage.*, 122(3), 214–217.
- Jowitt, P. W., and Xu, C. (1990). "Optimal valve control in water distribution networks." *J. Water Resour. Plann. Manage.*, 116(4), 455–472.
- Kalungi, P., and Tanyimboh, T. (2003). "Redundancy model for water distribution systems." *Reliab. Eng. Syst. Saf.*, 82(3), 275–286.
- Kettler, A. J., and Goulter, I. C. (1985). "An analysis of pipe breakage in urban water distribution networks." *Can. J. Civ. Eng.*, 12, 286–293.
- Kleiner, Y., and Rajani, B. B. (2001). "Comprehensive review of structural deterioration of water mains: Statistical models." *Urban Water*, 3(3), 121–150.
- Kleiner, Y., and Rajani, B. B. (2002). "Forecasting variations and trends in water-main breaks." *J. Infrastruct. Syst.*, 8(4), 122–131.
- Lambert, A. O. (1994). "Accounting for losses: The bursts and background concept (BABE)." *J. Inst. Water Environ. Manage.*, 8(2), 205–214.
- Lambert, A. O. (2001). "What do we know about pressure: Leakage relationships in distribution systems?" *Proc., IWA Conf. on System Approach to Leakage Control and Water Distribution Systems Management*.
- Lambert, A. O., and Hirner, W. (2000). *The blue pages*, IWA Publishing, London, U.K.
- May, J. (1994). "Pressure dependent leakage." *World Water Environmental Engineering Management*.
- McKay, M. D., Conover, W. J., and Beckman, R. J. (1979). "A comparison of three methods for selecting values of input variables in the analysis of output from a computer code." *Technometrics*, 211, 239–245.
- Rossman, L. A. (2000). *EPANET 2 user's manual*, U.S. Environmental Protection Agency, Cincinnati.
- Savic, D. A., and Walters, G. A. (1997). "Genetic algorithms for the least-cost design of water distribution networks." *J. Water Resour. Plann. Manage.*, 123(2), 67–77.
- Shamir, U., and Howard, C. D. D. (1979). "An analytic approach to scheduling pipe replacement." *J. Am. Water Works Assoc.*, 117(5), 248–258.
- Todini, E. (2003). "A more realistic approach to the "extended period simulation" of water distribution networks." *Advances in water supply management*, C. Maksimovic, D. Butler, and F. A. Memon, eds., Balkema, Lisse, The Netherlands, 173–184.
- Todini, E., and Pilati, S. (1988). "A gradient algorithm for the analysis of pipe networks." *Computer applications in water supply (Systems analysis and simulation)*, B. Coulbeck, and C. H. Orr, eds., Vol. 1, Wiley, London, 1–20.
- Vairavamoorthy, K., and Lumbers, J. (1998). "Leakage reduction in water distribution systems: optimal valve control." *J. Hydraul. Eng.*, 124(9), 1146–1154.
- Wagner, J. M., Shamir, U., and Marks, D. H. (1988). "Water distribution reliability: Simulation methods." *J. Water Resour. Plann. Manage.*, 114(3), 276–294.
- Walski, T. M. (1987). "Replacement rules for water mains." *J. Am. Water Works Assoc.*, 79(9), 33–38.
- Walski, T. M., and Pelliccia, A. (1982). "Economics analysis of water main breaks." *J. Am. Water Works Assoc.*, 74(3), 140–147.
- Wu, Z. Y., Wang, R. H., Walski, T. M., Yang, S. Y., and Boudler, D. (2006). "Efficient pressure dependent demand model for large water distribution system analysis." *Proc., 8th Water Distribution System Analysis Symp. (CD-ROM)*, <http://scitation.aip.org>.